Different complex regulatory phenotypes underlie hybrid male sterility in divergent rodent crosses

Kelsie E. Hunnicutt[*,1], Colin Callahan[2], Sara Keeble[2], Emily C. Moore[1,2], Jeffrey M. Good[2], and Erica L. Larson[*,1]

[1] University of Denver, Department of Biological Sciences, Denver, CO, 80208
[2] Division of Biological Sciences, University of Montana, Missoula, MT, 59812
*Corresponding authors

ORCID: 0000-0002-9674-0630 (KEH)
ORCID: 0000-0002-0385-1121 (CC)
ORCID: 0000-0002-7318-3122 (SK)
ORCID: 0000-0001-6166-3367 (ECM)
ORCID: 0000-0003-0707-5374 (JMG)
ORCID: 0000-0003-3006-645X (ELL)

Corresponding Authors:
Kelsie Hunnicutt
Department of Biological Sciences
University of Denver
Denver, CO 80208
Email: Kelsie.Hunnicutt@du.edu

Erica Larson
Department of Biological Sciences
University of Denver
Denver, CO 80208
Email: Erica.Larson@du.edu

Running title: Rodent hybrid male sterility

Key words: speciation, hybrid male sterility, gene expression, fluorescence activated cell sorting, meiotic sex chromosome inactivation, *Phodopus*

ABSTRACT

Hybrid incompatibilities are a critical component of species barriers and may arise due to negative interactions between divergent regulatory elements in parental species. We used a comparative approach to identify common themes in the regulatory phenotypes associated with hybrid male sterility in two divergent rodent crosses, dwarf hamsters and house mice. We investigated three potential characteristic regulatory phenotypes in hybrids including the propensity towards over or underexpression relative to parental species, the influence of developmental stage on the extent of misexpression, and the role of the sex chromosomes on misexpression phenotypes. In contrast to near pervasive overexpression in hybrid house mice, we found that misexpression in hybrid dwarf hamsters was dependent on developmental stage. In both house mouse and dwarf hamster hybrids, however, misexpression increased with the progression of spermatogenesis, although to varying extents and with potentially different consequences. In both systems, we detected sex-chromosome specific overexpression in stages of spermatogenesis where inactivated X chromosome expression was expected, but the hybrid overexpression phenotypes were fundamentally different. Importantly, misexpression phenotypes support the presence of multiple histological blocks to spermatogenesis in dwarf hamster hybrids, including a potential role of meiotic stalling early in spermatogenesis. Collectively, we demonstrate that while there are some similarities in hybrid regulatory phenotypes of house mice and dwarf hamsters, there are also clear differences that point towards unique mechanisms underlying hybrid male sterility in each system. Our results highlight the potential of comparative approaches in helping to understand the importance of disrupted gene regulation in speciation.

INTRODUCTION

The evolution of postzygotic reproductive barriers, such as hybrid inviability and sterility, is an important part of the speciation process, and identifying the genetic architecture of hybrid incompatibilities has been a common goal uniting speciation research (Coughlan and Matute 2020). While identifying the genetic basis of hybrid dysfunction remains difficult in many systems, downstream regulatory phenotypes can provide insight into the underlying mechanisms of speciation (Mack and Nachman 2017). An outstanding question surrounding the role of disrupted gene regulation and speciation is whether the combination of two divergent genomes in hybrids results in expression perturbations that are consistent or repeatable across species. At the broadest level, it is unclear whether hybrids tend to have over or underexpression of genes relative to parental species (Ortíz-Barrientos et al. 2007), and whether misexpression is modulated by cis or trans regulatory elements (Wittkopp et al. 2004; McManus et al. 2010; Oka et al. 2014; Mack et al. 2016; Mugal et al. 2020; Kopania, Larson, et al. 2022). We might predict that misexpression in hybrids would be biased towards overexpression if hybrid incompatibilities disrupt gene repression (Meiklejohn et al. 2014; Barreto et al. 2015; Larson et al. 2017). Alternatively, expression in hybrids may tend towards underexpression if transcription factor binding with promoter or enhancer elements is impaired (Oka et al. 2014; Guerrero et al. 2016) or if divergence stimulates epigenetic silencing (Paun et al. 2007; Shivaprasad et al. 2012; Lafon-Placette and Köhler 2015; Zhu et al. 2017). At a finer scale, misexpression may depend on developmental stage: for example, if there is greater pleiotropy earlier in development (Ortíz-Barrientos et al. 2007; Cutter and Bundus 2020). In particular, we might expect sterile hybrids to have more misexpression during later stages of gametogenesis when genes are evolving rapidly and are potentially under less regulatory constraint (Kopania, Larson, et al. 2022; Murat et al. 2023). Finally, the role of sex chromosome regulation in inviable or sterile hybrids encompasses both of these larger questions. Sex

chromosomes may be prone to asymmetry in their expression divergence (Oka and Shiroishi 2014; Civetta 2016) and be regulated differently across different stages of development (Presgraves 2008; Larson et al. 2018), particularly in reproductive tissues, and thus may play a central role in hybrid dysregulation relative to autosomes.

Disruption of sex chromosome regulation is thought to be a potentially widespread regulatory phenotype in sterile hybrids (Lifschytz and Lindsley 1972; Larson et al. 2018), in part because X chromosome repression may be crucial to normal spermatogenesis in diverse taxa (McKee and Handel 1993; Landeen et al. 2016; Taxiarchi et al. 2019; Rappaport et al. 2021; Viera et al. 2021; Murat et al. 2023). Furthermore, misregulation of the X chromosome is associated with hybrid sterility in several species pairs (Davis et al. 2015; Bredemeyer et al. 2021; Sánchez-Ramírez et al. 2021), although it has been best studied in house mice. In fertile male mice, the X chromosome is silenced early in meiosis through meiotic sex chromosome inactivation (MSCI; McKee and Handel 1993; Handel 2004) and is again repressed in postmeiotic sperm development (*i.e.,* postmeiotic sex chromosome repression or PSCR; Namekawa et al. 2006). In contrast, the X chromosome is not properly inactivated and is overexpressed in sterile hybrid mice (Good et al. 2010; Bhattacharyya et al. 2013; Campbell et al. 2013; Turner et al. 2014; Larson et al. 2017; Larson et al. 2022). Disrupted MSCI in house mice is associated with divergence at *Prdm9*, a gene that is a major contributor to hybrid male sterility (Mihola et al. 2009; Davies et al. 2016). However, misexpression of the X chromosome in sterile hybrids could result from mechanisms other than *Prdm9*-associated disrupted MSCI, such as mispairing of the sex chromosomes due to divergence in their region of homology known as the pseudoautosomal region (PAR; Burgoyne 1982; Ellis and Goodfellow 1989; Raudsepp and Chowdhary 2015). In sum, the ubiquity of X chromosome repression and the growing body of evidence linking disrupted MSCI to hybrid sterility in mammals suggest that

disrupted sex chromosome regulation may be a common regulatory phenotype in sterile hybrid males.

Here, we characterized disruption of gene regulation associated with hybrid male sterility in two rodent crosses, dwarf hamsters and house mice, which span ~35 million years of divergence (Swanson et al. 2019). The regulatory phenotypes of hybrid male sterility have been thoroughly studied in house mice (Good et al. 2010; Bhattacharyya et al. 2013; Campbell et al. 2013; Turner et al. 2014; Larson et al. 2017; Hunnicutt et al. 2022; Larson et al. 2022). We contrast these with an analogous cross between two sister species of dwarf hamster, Campbell's dwarf hamster (*Phodopus campbelli*) and the Siberian dwarf hamster (*P. sungorus*), and their sterile F1 hybrid male offspring. These species diverged only ~0.8-1.0 million years ago (Neumann et al. 2006), and they are not thought to interbreed in the wild due to geographic separation (Ishishita et al. 2015). Crosses between female *P. sungorus* and male *P. campbelli* produce sterile hybrid males that, similar to mice, have a range of sterility phenotypes, suggesting multiple histological blocks to spermatogenesis (Ishishita et al. 2015; Bikchurina et al. 2018). Hybrids from the reciprocal cross are usually inviable due to abnormal growth in utero (Brekke and Good 2014). Intriguingly, the species origin of the X chromosome is the primary genetic factor controlling hybrid inviability (Brekke et al. 2021). The frequently observed asynapsis of the sex chromosomes in hybrid dwarf hamsters provide additional reason to think that X chromosome-specific misregulation may be observed in sterile hybrid dwarf hamsters (Ishishita et al. 2015; Bikchurina et al. 2018). The combination of these abnormal histological phenotypes and the interactions between diverse reproductive barriers make dwarf hamsters an important comparison to mice for investigating what regulatory phenotypes may be associated with reproductive isolation between species.

Regulatory phenotypes associated with hybrid sterility have historically been difficult to assess because the cellular diversity of reproductive tissues (*e.g.,* testes; Ramm and Schärer

2014) confounds inferences of gene expression (Good et al. 2010; Montgomery and Mank 2016; Hunnicutt et al. 2022), thus requiring molecular approaches that permit greater spatial and developmental resolution. To overcome these difficulties, we used Fluorescence Activated Cell Sorting (FACS) to isolate and sequence cell populations across the developmental timeline of spermatogenesis for each species pair and their F1 hybrids, including stages that span the different sex chromosome regulatory states. We used both datasets to address three main questions about the regulatory phenotypes observed in sterile hybrids: (1) does misexpression tend towards up- or downregulation in hybrids compared to parents? (2) are there similar patterns of disrupted expression across stages of development? and (3) is there a clear differentiation between autosomes and sex chromosomes in regulatory phenotype? And if so, is sex chromosome specific misexpression consistent with either disrupted MSCI and/or disrupted PAR regulation? Collectively, we demonstrate the power of cell-specific approaches for untangling the regulatory phenotypes associated with the evolution of hybrid male sterility and for identifying common themes in the mechanistic basis of hybrid incompatibilities across divergent taxa.

RESULTS

Impaired sperm production in hybrid male dwarf hamsters

We first established the extent of hybrid male sterility in dwarf hamsters by comparing reproductive phenotypes for *P. campbelli*, *P. sungorus*, and F1 hybrid males (Figure 1; Table S1). *Phodopus sungorus* males had smaller testes and seminal vesicles than *P. campbelli* males (Dunn's Test relative testes weight $p < 0.001$; relative seminal vesicle weight $p = 0.0061$; Figure 1), perhaps reflecting inbreeding depression on this laboratory colony. However, these species did not differ in normalized sperm counts ($p = 0.071$) or in sperm motility ($p = 0.12$). The F1 hybrid males exhibited extreme reproductive defects relative to *P. campbelli* (Figure 1).

Hybrid males had smaller testes ($p < 0.001$) and seminal vesicles ($p < 0.001$) than male *P. campbelli* hamsters, and importantly, produced almost no mature spermatozoa. In the one instance where a hybrid male produced a single mature spermatozoon, it was non-motile, indicating severe reproductive impairment in hybrid males. Overall, our results confirmed previous reports of reduced fertility in hybrid male dwarf hamsters (Ishishita et al. 2015; Bikchurina et al. 2018).

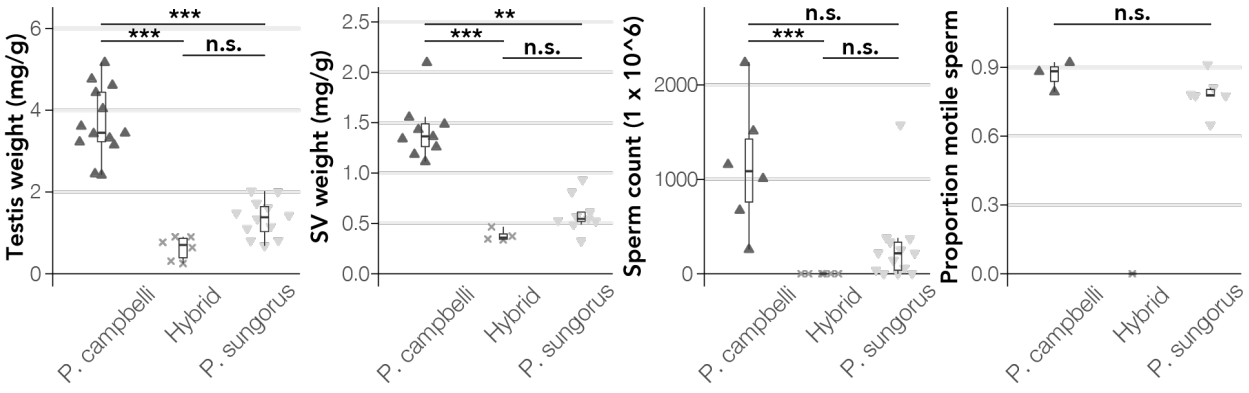

Figure 1. Hybrid dwarf hamsters exhibit multiple sterility phenotypes. We assessed paired testes weight and paired seminal vesicle weight (SV), both normalized by body weight, sperm count, and proportion of motile sperm for *P. sungorus*, *P. campbelli*, and F1 hybrids. Whiskers extend to either the largest or smallest value or no further than 1.5 times the interquartile range, and *** indicates $p < 0.001$, ** indicates $p < 0.01$, and n.s. indicates non-significant difference between means at $p > 0.05$ using a post-hoc Dunn's test with FDR correction. Upwards-pointing triangles (▲) indicate *P. campbelli*, downwards-pointing triangles (▼) indicate *P. sungorus*, and crosses (✖) indicate F1 hybrids.

139 **Cell-specific gene expression across spermatogenesis**

140 To characterize cell-specific gene expression, we used FACS to isolate enriched cell
141 populations from each fertile parent species and their sterile F1 hybrids across four stages of
142 spermatogenesis. The four targeted populations included: spermatogonia (mitotic precursor
143 cells), leptotene/zygotene spermatocytes (meiotic cells before MSCI), diplotene spermatocytes
144 (meiotic cells after MSCI), and round spermatids (postmeiotic cells). We were unable to isolate
145 round spermatids from the F1 hybrids, which was consistent with the lack of mature
146 spermatozoa present in the cauda epididymis extractions (Figure 1). We sequenced RNA from
147 each cell population for *P. campbelli* (spermatogonia n = 4, leptotene/zygotene n = 5, diplotene
148 n = 5, and round spermatids n = 4; Table S2), *P. sungorus* (spermatogonia n = 4,
149 leptotene/zygotene n = 4, diplotene n = 5, and round spermatids n = 3), and F1 hybrid males (
150 *P. campbelli* ♀ x *P. sungorus* ♂; spermatogonia n = 4, leptotene/zygotene n = 4, diplotene n =
151 4). We compared our hamster expression data to an analogous cell-specific RNASeq dataset
152 from two species of house mice, *Mus musculus musculus* and *M. m. domesticus*, and their
153 sterile F1 hybrids (Larson et al. 2017).

154 We used two approaches to evaluate the purity of spermatogonia, leptotene/zygotene
155 spermatocytes, diplotene spermatocytes, and round spermatids isolated from males from both
156 parental species: (1) quantifying the relative expression of a panel of cell population marker
157 genes and (2) characterizing the expression patterns of the sex chromosomes across
158 development. We found that our candidate marker genes had the highest expression in their
159 expected cell population for all stages except leptotene/zygotene (Figures S4 and 5), indicating
160 high purity of spermatogonia, diplotene spermatocytes, and round spermatids.
161 Leptotene/zygotene markers did not have the highest expression in leptotene/zygotene
162 samples (except for *Ccnb1ip1*), potentially indicating lower purity of this cell population.
163 Nonetheless, the patterns of X chromosome expression in fertile parents was consistent with

expectations across this developmental timeline: the X chromosome had active expression in spermatogonia and leptotene/zygotene cells, was inactivated in diplotene cells consistent with MSCI, and was partially inactivated in round spermatids, consistent with PSCR (Figure 2; Namekawa et al. 2006), indicating successful isolation of these cell populations. When we examined overall expression differences among dwarf hamsters, we found that samples separated primarily by cell population, then by species within a cell population, with a lack of clear separation of spermatogonia and leptotene/zygotene samples but distinct populations of diplotene and round spermatids (Figure 3). Hybrids showed intermediate expression level relative to parent species for all cell populations (Figures S2 and 3). The expression profiles of hybrid diplotene cells ranged from clustering with parental leptotene/zygotene to parental diplotene cells, which contrasted with what we observed in house mice where hybrid diplotene cells clustered distinctly with parental diplotene cells (Figure 3). Overall, our results indicate that we successfully isolated cell populations in parental dwarf hamsters that span the full extent of spermatogenesis.

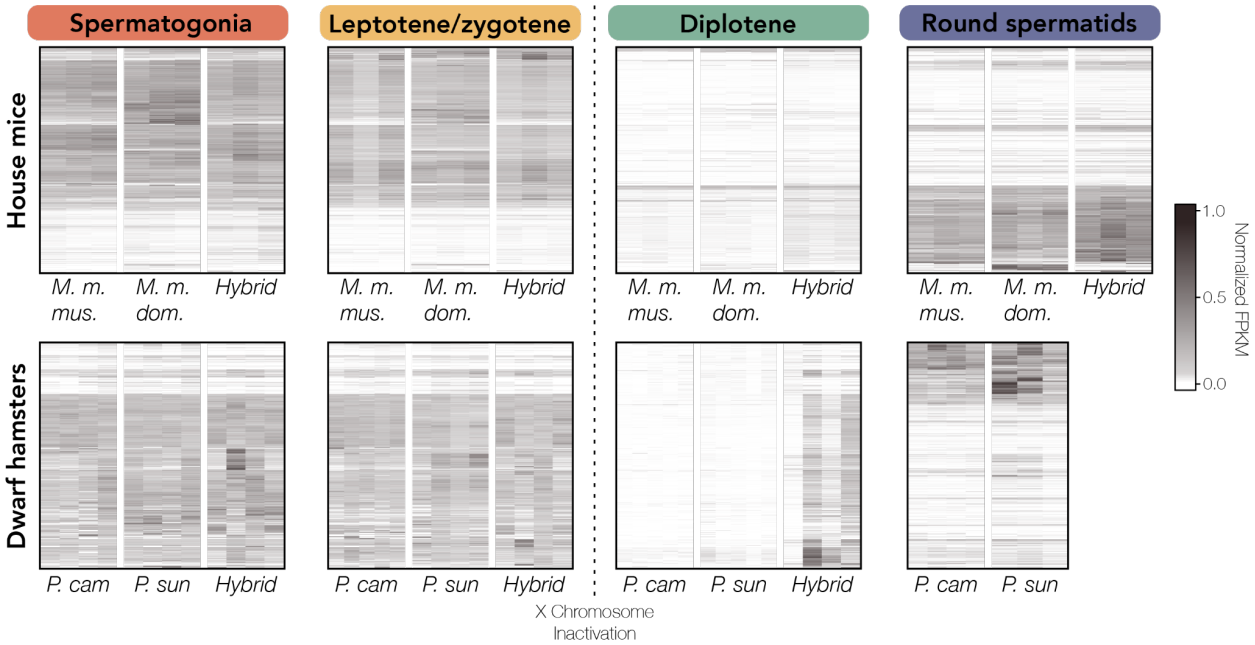

Figure 2. Overexpression of X-linked genes in diplotene spermatocytes in both house mouse and dwarf hamster hybrids. Heatmap of X-linked gene expression in house mice (upper panel) and dwarf hamsters (lower panel) plotted as normalized FPKM values that are hierarchically clustered using Euclidean distance. Each column represents a different individual, each row represents a gene, and darker colors indicate higher expression. The heatmap was generated with the R package ComplexHeatmap v.2.12.0 (Gu et al. 2016). Note, hybrid dwarf hamsters do not produce mature spermatozoa, and accordingly, we were unable to isolate round spermatids.

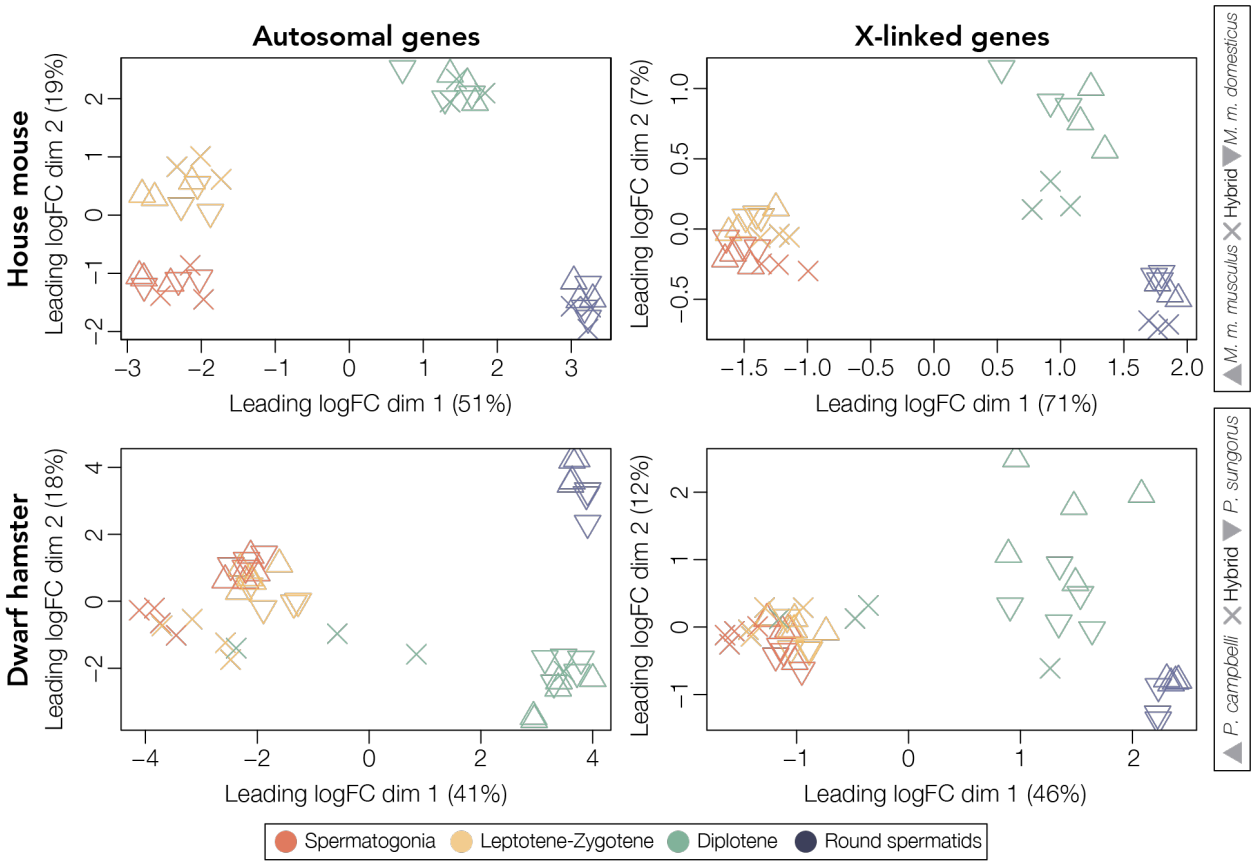

Figure 3. Hybrid gene expression profiles cluster by parental spermatogenic cell population in house mice but not dwarf hamsters. Multidimensional scaling (MDS) plots of distances among house mouse (upper panels) and dwarf hamster (lower panels) samples for expressed autosomal (left) and X-linked (right) genes. Distances are calculated as the root-mean-square deviation (Euclidean distance) of log2 fold changes among genes that distinguish each sample. Each species and F1 hybrid is indicated by a symbol, and samples are colored by cell population.

Disrupted transcriptional activation early in spermatogenesis in dwarf hamsters

We sought to characterize which regulatory phenotypes were associated with sterile hybrids in both house mice and dwarf hamsters. We first investigated whether misexpression tends towards up- or downregulation in hybrids compared to parents [measured as the log fold

change (logFC) in expression between hybrids and parents sharing the same X chromosome for differentially expressed (DE) genes]. Misexpression in hybrid house mice was biased towards upregulation across spermatogenesis in sterile hybrids (average logFC of spermatogonia autosomal DE genes: +1.17/ (X^2): $p < 0.001$; diplotene: +1.13/ (X^2): $p < 0.001$; Figure 4), as was X-linked misexpression (spermatogonia average logFC: +1.63/ (X^2): $p < 0.001$; leptotene/zygotene: +1.20 (X^2): $p < 0.001$; diplotene: +2.54/ (X^2): $p < 0.001$), with only the exception of autosomal leptotene/zygotene DE genes (leptotene/zygotene: +0.49/ (X^2): $p = 0.408$). In contrast, we found that the direction of misexpression in dwarf hamster hybrids was stage-specific. Differentially expressed autosomal genes in dwarf hamster hybrids were overwhelmingly downregulated in both early stages of spermatogenesis especially in comparison to house mice (average logFC of spermatogonia autosomal DE genes: -2.63/ (X^2): $p < 0.001$; leptotene/zygotene: -1.73/ (X^2): $p < 0.001$; Figure 4) but upregulated in diplotene (average logFC = +2.15/ (X^2): $p < 0.001$; Figure 4). When comparing both X-linked and autosomal expression in dwarf hamsters, we found similar patterns: almost all differentially expressed X-linked genes in the first two stages of spermatogenesis were exclusively downregulated (spermatogonia average logFC = -6.50/ (X^2): $p < 0.001$; leptotene/zygotene: -5.44/ (X^2): $p < 0.001$), and differential X-linked expression in diplotene was biased towards upregulation (average logFC: 5.57/ (X^2): $p < 0.001$). These patterns held regardless of which parent species was used as a contrast for dwarf hamsters (Figure S6). When hybrid house mice were compared with the parent species with a different X chromosome (*M. m. domesticus*), the direction of misexpression was positive for autosomal and X-linked spermatogonia and diplotene, as in the comparisons with *M. m. musculus*, but negative for autosomal and X-linked leptotene/zygotene.

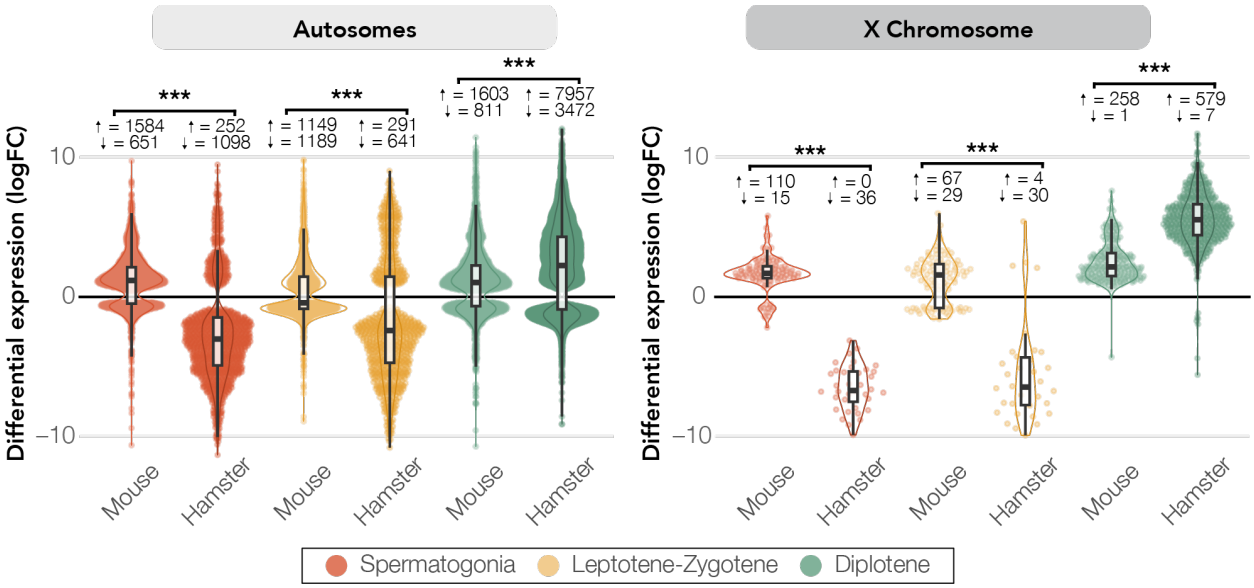

Figure 4. House mice and dwarf hamster hybrids have opposite patterns of disrupted regulation early in spermatogenesis. logFC of differentially expressed genes between hybrids and their parent species with the same X chromosome (*i.e.,* hybrids versus *M. m. musculus* mice; hybrid versus *P. campbelli* dwarf hamsters) for each stage. Results are displayed for autosomes (left) and the X chromosome (right). *** indicates $p < 0.001$ for pairwise comparisons from Wilcoxon signed-rank tests after FDR correction. Whiskers extend to either the largest or smallest value or no further than 1.5 times the interquartile range. The number of up and downregulated differentially expressed genes in hybrids are listed next to arrows indicating direction of differential expression.

Second, we investigated how developmental stage influenced the extent of hybrid misexpression. For both dwarf hamsters and house mice, misregulation in hybrids increased with the progression of spermatogenesis, though to a greater extent in dwarf hamsters (Figure S9). In dwarf hamsters, there were substantially more differentially expressed genes in diplotene spermatocytes than earlier stages of spermatogenesis (spermatogonia = 1,386, leptotene/zygotene = 966, and diplotene = 12,015 genes). In mice, there was also a trend

245 towards misexpression late, although it was not as dramatic as in dwarf hamsters
246 (spermatogonia = 2,360, leptotene/zygotene = 2,434, diplotene = 2,673, and round spermatids
247 = 4,181 genes). We also found a much greater genome-wide disruption of expression in
248 diplotene cells of dwarf hamsters - nearly half the transcriptome was misexpressed (Figures
249 S7-S9), indicating more widespread regulatory disruption than was observed in house mouse
250 hybrids.

251 To determine if the differences we observed in the extent of misregulation between
252 dwarf hamsters and house mice was due to greater expression variability across our dwarf
253 hamster samples, we calculated the Biological Coefficient of Variation (BCV), a measurement
254 of inter-replicate variability, for each species and hybrid across the first three cell populations.
255 Inter-replicate variability was higher in dwarf hamster hybrids relative to house mouse hybrids
256 (dwarf hamsters BCV = 0.69; house mice = 0.18). However, the extent of the variability
257 observed in hybrids relative to the inter-replicate variability of parental species differed
258 between house mice and dwarf hamsters: dwarf hamster hybrid variability was less than dwarf
259 hamster parental samples (*P. campbelli* = 0.49; *P. sungorus* = 0.40), but hybrid variability was
260 similar to parental samples for house mice (*M. m. musculus* = 0.19; *M. m. domesticus* = 0.22).
261 The greater inter-replicate variability in dwarf hamster hybrids relative to parent species
262 suggests that the increased misexpression we see in hybrids cannot be explained by greater
263 inter-replicate variability in our dwarf hamster samples. Thus, while there were hints of
264 disruption early in spermatogenesis in both mouse and dwarf hamster hybrids, misexpression
265 was amplified across the developmental timeline in both species.

266 Third, we characterized whether there was a clear difference between the autosomes
267 and sex chromosomes in regulatory phenotype. Across all stages of spermatogenesis in house
268 mice, autosomal expression is relatively unperturbed in contrast to greatly disrupted sex
269 chromosome expression (Figure 4). Surprisingly, misregulation in dwarf hamsters early in

270 spermatogenesis was not sex chromosome-specific, as the sex chromosomes in dwarf
271 hamsters showed no over-enrichment for differentially expressed genes early in
272 spermatogenesis between parent species and hybrids (spermatogonia: $p = 0.995$;
273 leptotene/zygotene: $p = 0.30$; Figure S7). However, we note that the magnitude of
274 misregulation was greater for sex chromosomes than autosomes in dwarf hamsters for both
275 spermatogonia and leptotene/zygotene (Figure 4; discussed above). Only one autosome
276 showed either over- or under-enrichment for differentially expressed genes in the first two cell
277 populations: over-enrichment of chromosome 11 in spermatogonia (hypergeometric test; $p =$
278 0.018) and leptotene/zygotene ($p = 0.017$; Figure S7). However, the X chromosome was
279 enriched for DE genes in diplotene cells in hybrid dwarf hamsters (observed X-linked DE genes
280 $= 585$; expected X-linked DE genes $= 247$; $p < 0.001$; Figure S7), consistent with sex
281 chromosome-specific misexpression in this cell population. In mice, the X chromosome was
282 over-enriched for differentially expressed genes between hybrids and parents for all stages
283 except leptotene/zygotene (spermatogonia $p = 0.001$; leptotene/zygotene $p = 0.436$; diplotene
284 $p < 0.001$; round spermatids $p < 0.001$; Figure S8), suggesting a difference in the extent of the
285 role for sex chromosome-specific disruption between systems.
286

287 **Misexpression in diplotene appears unrelated to disrupted MSCI in dwarf hamsters**

288 We next asked whether similar disrupted regulatory processes resulted in sex
289 chromosome-specific misexpression in both systems. In sterile hybrid house mice, X-linked
290 genes were upregulated during diplotene relative to autosomal genes (Wilcoxon signed rank
291 test: $p < 0.001$; Figure 2), consistent with disrupted MSCI (Good et al. 2010; Bhattacharyya et
292 al. 2013; Campbell et al. 2013; Turner and Harr 2014; Larson et al. 2017; Larson et al. 2022). In
293 sterile dwarf hamster hybrids, we also found that X-linked genes were upregulated during
294 diplotene relative to autosomal genes (Wilcoxon signed rank test: $p < 0.001$), but the extent of

295 X chromosome overexpression was greater than in hybrid house mice (average logFC X-linked
296 genes dwarf hamster: 5.57; house mice: 2.54; Wilcoxon signed rank test: $p < 0.001$; Figure 2).
297 There was also more variability in the relative extent of overexpression of X-linked genes in
298 hybrid dwarf hamsters during diplotene compared to the mean expression of X-linked genes of
299 parental dwarf hamsters (relative overexpression = 18.5 +/- 6.8) compared to hybrid house
300 mice (relative overexpression = 1.75 +/- 0.09; Figures 2 and S10). Strikingly, some hybrid male
301 dwarf hamsters had an almost completely silenced X chromosome, while others had an almost
302 completely transcriptionally-activated X chromosome (Figure 2).

303 Despite overexpression of the X chromosome during diplotene in hybrid dwarf
304 hamsters, the overall regulatory phenotype, including the identity and the extent of
305 misexpression of overexpressed genes, appeared to fundamentally differ between house
306 mouse and dwarf hamster hybrids (Figures 2 and 5). We established these differences in X-
307 linked overexpression using two approaches. First, we tested which parental cell types had the
308 highest expression correlation with hybrid diplotene cell types for both X-linked and autosomal
309 genes. In mice, the expression profile of X-linked genes in hybrids during diplotene was most
310 positively correlated with the expression profile of X-linked parental round spermatid genes,
311 consistent with disrupted MSCI (spermatogonia $(r) = -0.25$, $p < 0.001$; leptotene/zygotene $(r) = -$
312 0.073, $p = 0.035$; round spermatid $(r) = 0.26$, $p < 0.001$; Figures 2 and 5A). Autosomal genes
313 showed no positive correlations with either spermatogonia ($r = -0.26$; $p < 0.001$),
314 leptotene/zygotene ($r = -0.040$; $p < 0.001$), or round spermatids ($r = -0.060$; $p < 0.001$; Figure
315 5). If the X-linked overexpression phenotype in dwarf hamsters was consistent with disrupted
316 MSCI, then we would also expect X-linked and autosomal expression profiles in hybrid
317 diplotene to follow the same patterns. In contrast to this prediction, hybrid dwarf hamster
318 diplotene expression profiles for both X-linked and autosomal genes had a positive correlation
319 with parental leptotene/zygotene (autosomal $(r) = 0.13$, $p < 0.001$; X-linked $(r) = 0.22$, $p < 0.001$)

320 and spermatogonia (autosomal *(r)* = 0.027, $p < 0.001$; X-linked *(r)* = 0.091, $p = 0.017$) and a
321 negative correlation with round spermatids (autosomal *(r)* = -0.30, $p < 0.001$; X-linked *(r)* = -
322 0.31, $p < 0.001$; Figure 5). These striking differences in the strength and direction of expression
323 profile correlations suggest that the regulatory mechanisms underlying the overexpression
324 phenotype of X-linked genes in sterile hybrids differed between house mice and dwarf
325 hamsters.

326 This difference in pattern was further supported when we compared which sets of
327 genes were overexpressed in hybrid diplotene. For this approach, we characterized which
328 stages of spermatogenesis genes were active in and characteristic of, then identified which X-
329 linked genes in hybrid diplotene were overexpressed (defined as genes with normalized
330 expression in the top 10% of X-linked genes), and finally compared which parental stages
331 overexpressed X-linked genes were characteristic of in both systems. Similar to our correlation
332 analysis, we found that in hybrid house mice, the genes that were overexpressed in diplotene
333 most closely resembled genes that characterize round spermatids in parental mice (56.6% of
334 genes), but that in hybrid dwarf hamsters, overexpressed diplotene genes resembled
335 spermatogonia and leptotene/zygotene specific genes (45.6% and 44.6% respectively; Figure
336 5C). Because of the overwhelming similarity of the hamster hybrid diplotene samples to
337 parental spermatogonia and leptotene/zygotene samples, we next performed gene ontology
338 (GO) enrichment analyses on the set of differentially expressed genes in hybrid diplotene
339 samples relative to *P. campbelli* diplotene samples to determine which biological processes
340 could be potentially contributing to this pattern. Three Biological Process GO terms were
341 significant after FDR correction: “negative regulation of cell proliferation”, “positive regulation
342 of gene expression”, and “positive regulation of cell migration” (Figure 5D and S11). The first
343 two GO terms were consistent with the patterns we observed in our hybrid dwarf hamster
344 samples: “negative regulation of cell proliferation” could explain the similarity of our dwarf

345 hamster hybrid diplotene samples to the earlier spermatogenic cell types, and “positive
346 regulation of gene expression” was consistent with the dramatic overexpression phenotype of
347 both autosomal and X-linked genes during this stage. Collectively, these results suggest that
348 the X-linked overexpression phenotype in sterile hybrid dwarf hamsters is inconsistent with
349 disrupted MSCI and is possibly related to a stalling of spermatogenesis between
350 leptotene/zygotene and diplotene during Prophase I.

351

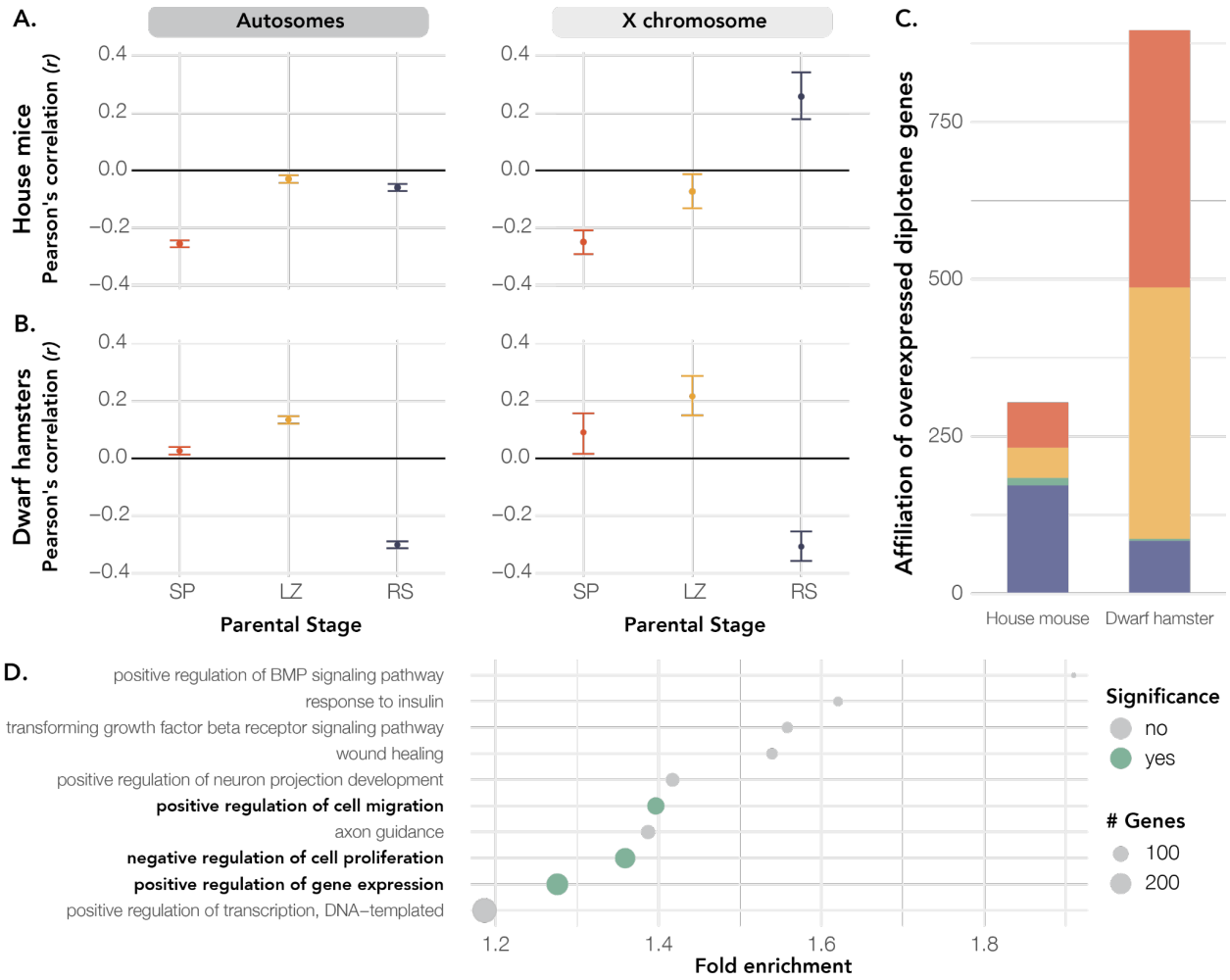

352

353 **Figure 5. Spermatogenesis in hybrid dwarf hamsters appears to stall after leptotene/**
354 **zygotene. A.** We calculated the Pearson’s correlation coefficient *(r)* between mean hybrid
355 diplotene expression and the mean expression for each parental cell type for both house mice

356 and **B.** dwarf hamsters. Correlation coefficients were calculated for both autosomal (left panels)
357 and X-linked (right panels) genes. We then generated bootstrap values by randomly sampling
358 the expression matrices for 1000 replicates. All values of *r* were significantly different from zero
359 ($p < 0.05$) after FDR correction. **C.** Classification of X-linked overexpressed genes in diplotene
360 cells of hybrid mice and dwarf hamsters by parental stage in which genes are induced.
361 Samples are colored by sample type (red = spermatogonia, yellow = leptotene/zygotene, green
362 = diplotene, and blue = round spermatids). **D.** The top 10 Biological Process GO terms (ranked
363 by FDR) for differentially expressed genes between hybrid dwarf hamsters and *P. campbelli* are
364 listed. Significant GO terms are colored while non-significant GO terms (FDR > 0.05) are gray.
365 Size of each point corresponds to the number of genes belonging to each GO term, and terms
366 are plotted by the fold enrichment of the GO term in the dataset relative to the provided gene
367 backgrounds.
368

369 **PAR expression was not disrupted in sterile hybrid dwarf hamsters**

370 Hybrid sterility in dwarf hamsters may be correlated with asynapsis of the X and Y
371 chromosomes because of divergence in the pseudoautosomal region (PAR) which prevents
372 proper chromosome pairing (Bikchurina et al. 2018). The PAR is the only portion of the sex
373 chromosomes that is able to synapse during routine spermatogenesis, and PAR genes are
374 assumed to escape silencing by MSCI (Raudsepp and Chowdhary 2015). However, because
375 XY asynapsis is common in dwarf hamster hybrids, Bikchurina et al. (2018) hypothesized that
376 MSCI may extend to the PAR of hybrid male dwarf hamsters, resulting in the silencing of PAR
377 genes in hybrids that may be critical to meiosis (Figure 6A). To test this hypothesis, we
378 compared the expression of genes located in the dwarf hamster PAR (Moore et al. 2022)
379 between parental dwarf hamster species and hybrid offspring across the timeline of
380 spermatogenesis. Specifically, we hypothesized that if XY asynapsis results in an extension of

381 MSCI to the PAR in hybrid dwarf hamsters, then hybrids should have similar PAR gene
382 expression to parents early in meiosis before homologous chromosome synapse during
383 pachytene. This should be followed by the silencing of PAR genes in hybrids, but not parent
384 species, during diplotene. If XY asynapsis does not alter the regulation of the PAR in hybrids,
385 then we may see two possible patterns. First, if all PAR genes are critical to the later stages of
386 spermatogenesis, then PAR genes in both hybrids and parents should be uniformly expressed
387 in diplotene. Alternatively, if PAR genes are not critical to the later stages of spermatogenesis,
388 then hybrids and parent species should have similar PAR gene expression, and not all PAR
389 genes may be expressed during diplotene.

390 We did not find evidence supporting PAR-wide silencing in dwarf hamster hybrids
391 during diplotene suggesting that MSCI is not extended to the PAR in dwarf hamster hybrids
392 because of XY asynapsis (Figure 6B). Furthermore, we also do not see PAR-wide expression of
393 genes during diplotene in hybrids or parents, indicating that not all PAR genes are critical to
394 the progression of spermatogenesis in dwarf hamsters. In general, most PAR gene expression
395 followed similar trends between hybrids and parent species. Three PAR genes were
396 differentially expressed between hybrids and *P. campbelli* during diplotene (*Ndrg2*,
397 Psun_G000022883, and Psun_G000022886; Table S3), but these genes were still expressed in
398 hybrids. Further, an association between PAR misregulation during the early stages of
399 spermatogenesis and hybrid male sterility also seems unlikely as only one gene, *Gprin1*,
400 showed consistent differential expression in early meiosis between both parent species and
401 hybrids (Table S3). Thus, based on the current annotation of the PAR in *P. sungorus*, we
402 currently find no direct evidence linking improper silencing of PAR genes to hybrid male sterility
403 in dwarf hamsters.
404

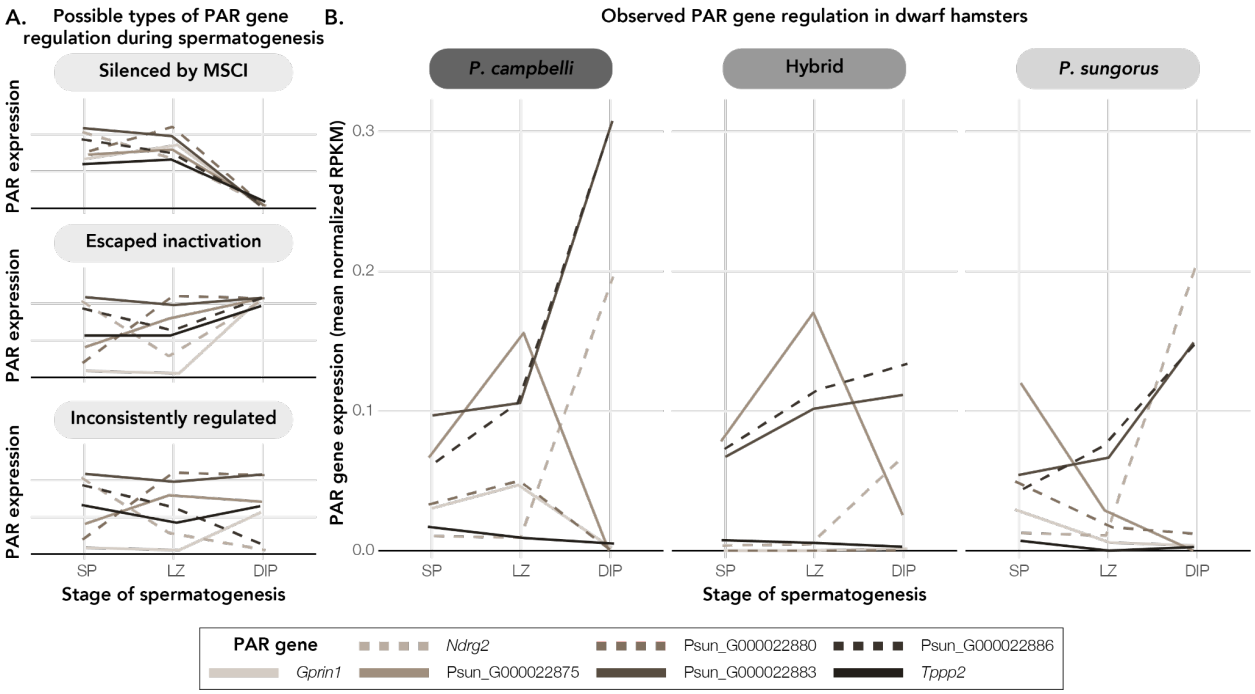

Figure 6. PAR gene expression is not disrupted during spermatogenesis in hybrid dwarf hamsters. A. Hypothesized types of PAR gene regulation across spermatogenesis. If MSCI extends to the entire X chromosome, then PAR genes would show some level of expression early in spermatogenesis which would then drop to zero in diplotene when MSCI occurs. If the PAR escapes silencing by MSCI and if PAR genes are critical to spermatogenesis, then we would expect PAR genes to be uniformly expressed in diplotene when the rest of the X chromosome is silenced. Finally, if the PAR escapes silencing by MSCI but all PAR genes are not critical to spermatogenesis, then we would expect some PAR genes to be expressed and some to be not expressed in diplotene. **B.** Observed patterns of PAR gene expression (as mean normalized RPKM across individuals) in parental species and hybrid dwarf hamsters for all PAR genes (indicated by line type and color) across spermatogenesis (SP = spermatogonia, LZ = leptotene/zygotene, and DIP = diplotene).

DISCUSSION

We used a comparative approach to understand common gene expression phenotypes associated with hybrid male sterility in two divergent rodent crosses. We characterized asymmetry of misexpression in hybrids, how misexpression changed over developmental timelines, and how the X chromosome and autosomes differed in both of these aspects. We found that while there were similarities in hybrid regulatory phenotypes in house mice and dwarf hamsters, there were also differences in the timing and chromosomal distribution of disrupted gene expression that point towards different underlying mechanisms behind hybrid male sterility.

Asymmetry and developmental timing of misexpression in hybrids

We first investigated patterns of gene misexpression in sterile male hybrids. Studies of misexpression in sterile or inviable hybrids have often focused on whether hybrid expression is biased towards over or underexpression, with the hypothesis that expression may be biased towards overexpression if hybrid incompatibilities disrupt repressive gene regulatory elements (Meiklejohn et al. 2014; Barreto et al. 2015; Larson et al. 2017). In house mice, there is strong support for overexpression of both autosomal and X-linked genes in sterile F1 hybrids (Mack et al. 2016; Larson et al. 2017; Hunnicutt et al. 2022; Larson et al. 2022), and further work has shown that F1 hybrid expression patterns depend on both autosomal background and sex chromosome mismatch (Kopania, Watson, et al. 2022). Surprisingly, we found that in dwarf hamster hybrids, there was nearly uniform downregulation of differentially expressed genes in mitotic cells and early meiotic cells, suggesting that a loss of regulatory repression is not an inevitable outcome of hybrid genomes. Asymmetric patterns of misexpression have been found in many hybrids, including underexpression in sterile *Drosophila* hybrids (Michalak and

443 Noor 2003; Haerty and Singh 2006; Llopart 2012) and sterile introgression lines of tomato
444 (Guerrero et al. 2016) and *Drosophila* (Meiklejohn et al. 2014), but overexpression has also
445 been found in other sterile hybrids (Llopart 2012; Davis et al. 2015). The variation we and
446 others have found in hybrid regulatory phenotypes suggests that the mechanisms of disrupted
447 expression are complex, even within groups with relatively shallow divergence times (such as
448 rodents), and we need more data from diverse hybrid sterility systems to begin to understand
449 common drivers of asymmetric hybrid misexpression.

450 The downregulation we observed in early spermatogenesis in hybrid dwarf hamsters
451 could be due to impaired transcription factor binding with promoter or enhancer elements (Oka
452 et al. 2014; Guerrero et al. 2016) or disrupted epigenetic silencing. Disruption of epigenetic
453 regulation of gene expression has been increasingly linked to hybrid dysfunction in plants
454 (Shivaprasad et al. 2012; Lafon-Placette and Köhler 2015; Zhu et al. 2017), especially
455 polyploids (Paun et al. 2007), and may also contribute to hybrid male sterility in *Drosophila*
456 (Bayes and Malik 2009) and cattle x yak hybrids (Luo et al. 2022). At least one known
457 chromatin difference has been documented between parental dwarf hamster species on the X
458 chromosome (Gamperl et al. 1977; Haaf et al. 1987). However, it is unknown if genome-wide
459 epigenetic regulatory mechanisms are disrupted in hybrid dwarf hamster spermatogenesis, and
460 further work is needed to distinguish between potential mechanisms underlying the observed
461 genome-wide downregulation.

462 Spermatogenesis as a developmental process may be sensitive to disruption (*i.e.,*
463 "faster male" evolution; Wu and Davis 1993), but it remains an open question whether specific
464 stages of spermatogenesis, or developmental processes more broadly, may be more prone to
465 the accumulation of hybrid incompatibilities. In general, earlier developmental stages are
466 thought to be under greater pleiotropic constraint and less prone to disruption (Cutter and
467 Bundus 2020). With the progression of mouse spermatogenesis, pleiotropy decreases (as

approximated by increases in tissue specificity; Murat et al. 2023) and the rate of protein-coding evolution increases (Larson et al. 2016; Kopania, Larson, et al. 2022; Murat et al. 2023), which may make the later stages of spermatogenesis more prone to accumulating hybrid incompatibilities. Indeed, we found fewer differentially expressed genes in sterile hybrids of both dwarf hamsters and house mice during the early stages of spermatogenesis than in later stages (Figures S7 and 8). Generally, there might be some tolerance for misregulation early in spermatogenesis, since misregulation of some genes during early stages does not always completely halt the progression of sperm development (Oka et al. 2010; Ishishita et al. 2015; Mipam et al. 2023). However, the patterns we find in dwarf hamsters suggests that spermatogenesis may be disrupted between zygotene and diplotene cell stages from early misexpression. Dwarf hamster hybrid diplotene cell populations had X-linked and autosomal gene expression profiles which more closely resemble parental leptotene/zygotene cell populations than either diplotene or postmeiotic cell populations. Furthermore, differentially expressed genes in hybrids during diplotene were enriched for genes associated with the GO term for “negative regulation of cell proliferation” suggesting that there may be a regulatory stalling of meiosis occurring in hybrid dwarf hamsters during early spermatogenesis. It’s unclear what underlying genomic mechanisms could result in this stalling, but it is possible that this disruption could potentially act as a major contributor to hybrid sterility in this system. Ultimately, we find that spermatogenesis is a complex and rapidly evolving developmental program that may provide many potential avenues across its timeline for the evolution of hybrid incompatibilities.

490 **Abnormal sex chromosome expression in dwarf hamster hybrids is inconsistent with**
491 **disrupted MSCI**

492 The sex chromosomes play a central role in speciation, an observation which has been
493 supported by both Haldane's rule (Haldane 1922) and the large X-effect on hybrid male sterility
494 (Coyne and Orr 1989). Misregulation of the X chromosome may contribute to hybrid sterility in
495 several species pairs (Davis et al. 2015; Morgan et al. 2020; Sánchez-Ramírez et al. 2021). The
496 X chromosome is transcriptionally repressed during routine spermatogenesis in many
497 organisms including eutherian mammals (McKee and Handel 1993), monotremes (Murat et al.
498 2023), *Drosophila* (Landeen et al. 2016), grasshoppers (Viera et al. 2021), mosquitos (Taxiarchi
499 et al. 2019), and nematodes (Rappaport et al. 2021). Because of the ubiquity of X chromosome
500 repression during spermatogenesis, disruption of transcriptional repression could be a
501 widespread regulatory phenotype in sterile hybrids (Lifschytz and Lindsley 1972; Larson et al.
502 2018). In sterile hybrid mice, disrupted X repression (disrupted MSCI) leads to the
503 overexpression of the normally silenced X chromosome, but not the autosomes, during
504 diplotene (Good et al. 2010; Bhattacharyya et al. 2013; Campbell et al. 2013; Turner and Harr
505 2014; Larson et al. 2017; Larson et al. 2022). We also found overexpression of the X
506 chromosome during diplotene in sterile hybrid dwarf hamsters, but in a manner inconsistent
507 with disrupted MSCI. Unlike in house mouse hybrids, both the X and autosomes are
508 overexpressed in dwarf hamster hybrid diplotene cells and the extent of X overexpression was
509 greater than what was observed in house mice, and importantly, more variable. In fact, some
510 dwarf hamster hybrids had wildly overexpressed X chromosomes while others appeared to
511 have properly silenced X chromosomes. Our expression correlation and gene set analyses of
512 hybrid diplotene cells provide additional evidence that the genes overexpressed in hybrid
513 hamster diplotene are different than those overexpressed in house mouse hybrids, sharing
514 more similarity to the earlier meiotic cell types than downstream postmeiotic cell types. Overall,

515 our results indicate fundamentally different patterns of X-linked overexpression in both
516 systems, with X-linked overexpression in dwarf hamster hybrids being inconsistent with
517 disrupted MSCI.

518 Much of what we know about the genomic architecture and the role of sex
519 chromosome misregulation in hybrid male sterility in mammals comes from decades of work
520 that have shown a major gene, *Prdm9*, and its X chromosome modulator, *Hstx2*, may be
521 responsible for most F1 hybrid male sterility in house mice (Forejt et al. 1991; Trachtulec et al.
522 1997; Mihola et al. 2009; Lustyk et al. 2019; Forejt et al. 2021). *Prdm9* directs the location of
523 double strand breaks during meiotic recombination (Mihola et al. 2009; Oliver et al. 2009;
524 Smagulova et al. 2016). In hybrid mice, divergence at *Prdm9* binding sites leads to asymmetric
525 double-stranded breaks and results in autosomal asynapsis, triggering Meiotic Silencing of
526 Unsynapsed Chromatin, shutting down transcription on asynapsed autosomes using the same
527 cellular machinery as MSCI (Turner 2015), and eventually meiotic arrest and cell death
528 (Bhattacharyya et al. 2013; Forejt et al. 2021). This process is associated with the disruption of
529 MSCI and a characteristic overexpression of the X chromosome during meiosis (Good et al.
530 2010; Bhattacharyya et al. 2013; Campbell et al. 2013; Turner and Harr 2014; Larson et al.
531 2017; Larson et al. 2022), but whether disrupted MSCI directly contributes to hybrid male
532 sterility or is simply a downstream consequence of *Prdm9* divergence is still uncertain (Forejt et
533 al. 2021).

534 Whether we should have expected patterns of disrupted sex chromosome expression
535 in sterile hybrid hamsters to be the same as house mice is unclear. The sex chromosomes in
536 pachytene cells of hybrid dwarf hamsters display normal yH2AFX staining (Ishishita et al. 2015;
537 Bikchurina et al. 2018), a key marker in MSCI (Abe et al. 2022), which may indicate that the
538 hybrid sex chromosomes are properly silenced. Additionally, autosomal asynapsis is rarely
539 observed in hybrid dwarf hamsters, and asynapsis is almost exclusive to the sex chromosomes

540 (Ishishita et al. 2015; Bikchurina et al. 2018). This contrasts *Prdm9*-mediated sterility in house
541 mice, where hybrid autosomes are often asynapsed and decorated with yH2AFX
542 (Bhattacharyya et al. 2013; Forejt et al. 2021). Mechanisms other than *Prdm9* may also disrupt
543 MSCI and result in sterility, such as macrosatellite copy number divergence (Bredemeyer et al.
544 2021) and X-autosome translocations that impair synapsis (Homolka et al. 2007), although
545 there is no evidence for X-autosome translocations between the two species of dwarf hamsters
546 (Moore et al. 2022). Thus, while MSCI may be a major target for the accumulation of
547 reproductive barriers between species in many mammalian systems, either through *Prdm9*
548 divergence or alternative mechanisms, our results suggest that sterility in dwarf hamsters has a
549 more composite regulatory basis.

550 Another mechanism often proposed to underlie mammalian male hybrid sterility,
551 especially in rodents, is divergence in the PAR between parental species. The PAR is the only
552 portion of the sex chromosomes which can synapse during spermatogenesis, and it is still
553 unclear if the regulation of the PAR is uniformly detached from MSCI across divergent
554 mammalian sex chromosome systems (Raudsepp and Chowdhary 2015). We find no evidence
555 that PAR-specific misregulation is associated with hybrid sterility in dwarf hamsters. PAR
556 genes are not silenced in hybrids or parents, a pattern that is inconsistent with MSCI that has
557 extended to the PAR due to XY asynapsis, and further, expression of PAR genes in hybrids
558 differs little from parental PAR expression. While we find no evidence that PAR misregulation
559 *per se* is associated with hybrid sterility in this system, we cannot rule out the possibility that
560 structural and sequence divergence between the PARs of *P. sungorus* and *P. campbelli* may
561 be associated with hybrid sterility. Structural and sequence divergence in the PAR has been
562 hypothesized to activate the meiotic spindle checkpoint by interfering with proper pairing of
563 sex chromosomes (Burgoyne et al. 2009; Dumont 2017). The PAR evolves rapidly in rodents
564 (White, Ikeda, et al. 2012; Raudsepp and Chowdhary 2015; Morgan et al. 2019), and this

elevated divergence may underlie sex chromosome asynapsis and apoptosis in several hybrid mouse crosses (Matsuda et al. 1991; Oka et al. 2010; White, Stubbings, et al. 2012; Dumont 2017). Furthermore, divergence in the mouse PAR has been implicated in spermatogenic defects in crosses where *Prdm9*-divergence is minimal, such as between closely related subspecies (Dumont 2017) or in mice with genetically-modified *Prdm9* alleles (Davies et al. 2021). Meiosis is likely tolerant to some degree of divergence in the PAR (Morgan et al. 2019), but exact limits are currently unknown. At this time, thorough analysis of structural and sequence divergence between the PARs in dwarf hamsters is challenging as the PAR is notoriously difficult to assemble (but see Kasahara et al. 2022), and there are annotation gaps in the current assembly of the PAR in dwarf hamsters. In sum, we find no clear pattern of regulatory disruption of PAR genes in sterile hybrid dwarf hamsters, though this result may change pending further refinement of the PAR annotation.

Conclusions

Cell-specific approaches for quantifying regulatory phenotypes are powerful tools for providing insight into the underlying mechanisms behind hybrid dysfunction (Hunnicutt et al. 2022), especially in systems where it remains difficult to interrogate the underlying genomic architecture of these traits. Using a contrast of dwarf hamster and house mouse hybrids, we have shown that transgressive overexpression is not an inevitable outcome of hybridization, that hybrid incompatibilities are likely to arise during multiple stages of spermatogenesis, and that disrupted sex chromosome silencing does not appear to play an equal role in sterility between these two systems. Both the regulatory phenotypes we observed here and histological evidence from other studies (Ishishita et al. 2015; Bikchurina et al. 2018) suggest that several reproductive barriers are acting during spermatogenesis in dwarf hamster hybrids. It has become increasingly apparent as more study systems are investigated that the genetic

basis of postzygotic species barriers are often complex and polymorphic (Cutter 2012; Coughlan and Matute 2020), and implementing approaches which account for the developmental complexities of hybrid dysfunction, as we have done here, will allow us to make further advances in understanding the processes of speciation.

MATERIALS AND METHODS

Hamster crosses and male reproductive phenotypes

We used wild-derived colonies of two sister species of dwarf hamster, *P. sungorus* and *P. campbelli*, established by Kathy Wynne-Edwards (Scribner and Wynne-Edwards 1994) and housed at the University of Montana. Both species were maintained as outbred colonies, but inbreeding levels of these closed colonies are still high (Brekke et al. 2018). We used males from both parent species and male F1 hybrid offspring from crosses of female *P. campbelli* with male *P. sungorus*. We weaned males in same-sex sibling groups between 17 and 21 dpp and housed them individually at 45 dpp. We euthanized reproductively mature males using carbon dioxide followed by cervical dislocation between 59 - 200 dpp (Table S1). All animal use was approved by the University of Montana (IACUC protocols 050-16JGDBS & 035-19JGDBS).

We measured several fertility metrics for parent species and hybrid males including paired testes weight, paired seminal vesicle weight, normalized sperm counts, and sperm motility (Good et al. 2008). Paired testes weight and paired seminal vesicle weight were correlated with body weight (paired testes weight Pearson's $r(29) = 0.47$, $p = 0.007$; paired seminal vesicle weight Pearson's $r(23) = 0.56$, $p = 0.003$), so we standardized both metrics relative to body weight. We calculated sperm count by isolating sperm from caudal epididymides diced in 1 ml of Dulbecco's PBS (Sigma) and incubated at 37°C for 10 minutes. We quantified sperm motility (proportion of motile sperm in a 5 µl suspension) and sperm count

614 (number of sperm with head and tail in a heat shocked 5 µl suspension) across a fixed area on
615 a Makler counting chamber. We performed statistical comparisons of fertility phenotypes in R
616 v.4.3.1, and we used the FSA package v.0.9.4 for the Kruskal-Wallis and Dunn's tests (Ogle
617 and Ogle 2017).
618

619 **Isolation of enriched cell populations from hamster testes**

620 To investigate the regulatory dynamics of the sex chromosomes during
621 spermatogenesis, we isolated four spermatogenic cell populations from whole testes using
622 FACS: spermatogonia, leptotene/zygotene spermatocytes, diplotene spermatocytes, and
623 round spermatids. Briefly, we disassociated a single testis per male following a published
624 protocol originally developed for house mice (Getun et al. 2011) with modifications
625 (github.com/goodest-goodlab/good-protocols/tree/main/protocols/FACS, last accessed June
626 16, 2021). We doubled the volumes of all reagents to account for the increased mass of testes
627 in dwarf hamsters relative to house mice. We isolated cell populations based on size,
628 granularity, and fluorescence on a FACSAria IIu cell sorter (BD Biosciences) at the University of
629 Montana Center for Environmental Health Sciences Fluorescence Cytometry Core. For each
630 sorted cell population, we extracted RNA using RNeasy kits (Qiagen) following protocols for
631 Purification of Total RNA from Animal Cells. We quantified sample RNA quantity and quality
632 (RNA integrity number > 7) on a Tapestation 2200 (Agilent) at the University of Montana
633 genomics core. RNA libraries were prepared by Novogene and sequenced on Illumina
634 NovaSeq 6000s (paired end, 150 bp). Six samples (distributed across different species and cell
635 types) had low RNA concentrations, and for these samples we used Novogene's low input
636 RNA library preparation (Table S2). MDS plots indicated no severe library batch effects
637 between samples from different library preparations (Figure S1) so we included all samples
638 from both libraries in subsequent analyses.

Read processing and mapping

We sequenced RNA from each cell population for three to five individuals of each parent species and F1 hybrids generating an average of ~27.5 million read pairs per individual (Table S2). We trimmed reads using Trimmomatic v.0.39 (Bolger et al. 2014) to remove low quality bases from the first and last 5 bp of each read and bases with an average Phred score of less than 15 across a 4 bp sliding window and only retained reads of at least 36 bp. We next used an approach (based on the modtools pipeline) which maps reads from each sample to pseudogenomes for both parent species (described below) to obtain a merged output alignment file in order to alleviate reference bias associated with mapping hybrids to only a single reference genome (Holt et al. 2013; Huang et al. 2014). For this approach, we mapped reads for each individual to both a *P. sungorus* pseudogenome and a *P. campbelli* pseudogenome with Hisat v.2.2.0 (Kim et al. 2019) with default settings and retaining at most 100 distinct, primary alignments. We generated the *P. sungorus* pseudogenome by mapping RNASeq reads from a male *P. sungorus* individual (30.6 million total read pairs; NCBI SRA: SRR17223284; Moore et al. 2022) to the *P. sungorus* reference genome with bwa-mem v.2.2.1 (Vasimuddin et al. 2019), and the *P. campbelli* pseudogenome by mapping female *P. campbelli* whole genome sequencing reads (average coverage: 33x; NCBI SRA: SRR17223279; Moore et al. 2022) to the *P. sungorus* reference genome. Because our *P. sungorus* pseudogenome was based on a male hamster and the reference genome on a female hamster, we excluded reads mapping to the PAR because sequences mapping to this region could have originated from either the X or Y chromosomes and interfered with subsequent variant calling. Following mapping, we used GATK v.4.2.5.0 HaplotypeCaller (-ERC GVCF) to call SNPs then performed genotyping with genotypeGVCFs. We hard-filtered our SNPs (--mask-extension 5 "QD < 2.0" "FS > 60.0" "MQ < 40.0" "QUAL < 30.0" "DP < 10" "DP > 150") and restricted SNPs to biallelic loci. Finally, we incorporated filtered SNPs back into the *P. sungorus* reference genome with

664 FastaAlternateReferenceMaker to create the *P. sungorus* and *P. campbelli* pseudoreferences.
665 For our RNASeq data, we appended query hit indexes to resulting alignment files using
666 hisat2Tophat.py (https://github.com/goodest-goodlab/pseudo-it/tree/master/helper-
667 scripts/hisat2Tophat.py, last accessed March 8th, 2022) to maintain compatibility with the
668 modtools pipeline. We used our vcfs (above) to generate a mod-file for both species with
669 vcf2mod from Lapels v.1.1.1 to convert alignments to the *P. sungorus* reference genome, and
670 Suspenders 0.2.6 to merge alignments while retaining the highest quality alignment per read
671 (Holt et al. 2013; Huang et al. 2014). We used featureCounts v.2.0.1 (Liao et al. 2014) to
672 estimate counts of read pairs that aligned to the same chromosome (-B and -C) and retained
673 only singly-mapped reads. Summaries of properly mapped reads for each sample can be
674 found in Table S2.

675 We sought to compare the gene expression phenotypes observed in dwarf hamsters to
676 those previously documented in house mice using published RNASeq data for the same four
677 spermatogenic cell types of two subspecies of house mouse and their sterile F1 hybrids
678 (Larson et al. 2017; Hunnicutt et al. 2022). These studies examined two subspecies of house
679 mice, *Mus musculus musculus* (intra-subspecific F1 males between wild-derived inbred strains
680 PWK/PhJ♀ and CZECHII/EiJ♂) and *M. m. domesticus* (intra-subspecific F1 males between
681 wild-derived inbred strains WSB/EiJ♀ and LEWES/EiJ♂) and their sterile (PWK♀ x LEWES♂)
682 F1 hybrids for disrupted gene expression across spermatogenesis following the same FACS
683 protocols implemented in this study. For all comparisons between house mice and dwarf
684 hamsters, we used read count files generated previously for house mice (Hunnicutt et al. 2022)
685 and performed all subsequent analyses in parallel for both systems.

686 **Gene expression pre-processing**

687 Following read processing and mapping, we conducted all analyses in R v.4.3.1. We
688 classified genes as “expressed” if genes had a minimum of one Fragment Per Kilobase of exon
689 per Million mapped reads (FPKM) in at least three samples, resulting in 21,077 expressed
690 genes across the whole dwarf hamster dataset and 21,212 expressed genes across the house
691 mouse dataset. We also identified sets of genes “induced” in a given cell-type defined as
692 genes with a median expression in a given cell population (normalized FPKM) greater than two
693 times its median expression across all other sorted cell populations (following Kousathanas et
694 al. 2014). We calculated normalized FPKM values by adjusting the sum of squares to equal one
695 using the R package vegan v.2.6-4 (Oksanen et al. 2013). We conducted expression analyses
696 using edgeR v.3.42.4 (Robinson et al. 2010) and normalized the data using the scaling factor
697 method (Anders and Huber 2010).

698 We assessed cell population purity using a panel of marker genes specific to the four
699 cell populations targeted by our FACS protocol and present in only a single copy in the *P.*
700 *sungorus* annotation. Spermatogonia markers included *Dmrt1* (Raymond et al. 2000) and *Hells*
701 (Green et al. 2018). Leptotene/zygotene markers included *Ccnb1ip1* and *Adad2* (Hermann et al.
702 2018). Diplotene was characterized by *Aurka* and *Tank* expression (Murat et al. 2023) and
703 round spermatids by *Cabyr* and *Acrv1* expression (Green et al. 2018). To estimate relative
704 purity, we quantified mean marker gene expression across replicates for a given cell population
705 for both parent species. A cell population was considered pure if it had higher marker gene
706 expression than other populations isolated by our FACS protocol and if X-linked gene
707 expression matched the expected regulatory dynamics (*i.e.,* active vs. silenced (MSCI) vs.
708 repressed (PSCR); Handel 2004; Namekawa et al. 2006). We examined expression patterns
709 across cell populations for all genes, autosomal genes, and X-linked genes using MDS plots
710 generated with the plotMDS function in limma v.3.56.2 (Ritchie et al. 2015) and heatmaps using

711 ComplexHeatmap v.2.16.0 (Gu et al. 2016). MDS plots used the top 500 genes with the largest
712 fold change difference between samples.
713
714 **Differential gene expression analysis**
715 We assessed differential gene expression by contrasting hybrids and each parent
716 species for all cell populations. We fit the expression data for dwarf hamsters and house mice
717 separately with negative binomial generalized linear models with Cox-Reid tagwise dispersion
718 estimates and adjusted P-values to a false discovery rate (FDR) of 5% (Benjamini and
719 Hochberg 1995). We quantified the biological coefficient of variation (BCV), a metric
720 representing the variation in gene expression among replicates (McCarthy et al. 2012), for each
721 dataset. Additionally, we calculated the BCV of just parental males or hybrid samples for each
722 species for the first three cell populations to examine whether dwarf hamster hybrids exhibited
723 more variability in expression than house mouse hybrids and parental dwarf hamsters. For our
724 differential expression analyses, we contrasted expression between hybrids and parents so
725 that a positive log fold-change (logFC) indicated overexpression in sterile males. Unless
726 otherwise specified, results discussed in the main text contrast hybrid offspring to the parent
727 with the same X chromosome (*P. campbelli* for dwarf hamster F1 hybrids and *M. m. musculus*
728 for house mouse F1 hybrids). Contrasts between F1 hybrids and *P. sungorus* or *M. m.*
729 *domesticus* are provided in supplementary material (Figures S6, 9, and 10).
730 We tested for significant differences in the number of under and overexpressed DE
731 genes within a stage for both house mouse and hamster hybrids using X^2 tests with chisq.tests
732 in R and used FDR correction for multiple comparisons. We also tested for differences in the
733 magnitude of misexpression between mouse and hamster hybrids for each stage by
734 comparing the distributions of the logFC of DE genes between hybrids and parent species
735 between mice and hamsters using Wilcoxon signed-rank tests and FDR correction. To

736 characterize hybrid diplotene expression in both house mice and dwarf hamsters, we used two
737 approaches. First, we calculated Pearson's correlation coefficient *(r)* between average
738 normalized hybrid diplotene expression and the average normalized expression in each
739 parental cell type. We corrected p-values for each correlation with FDR. We generated
740 bootstrap values for each correlation coefficient by randomly sampling the expression matrices
741 with replacement for each sample type for 1000 replicates. Second, we compared the gene
742 sets that escaped MSCI in each species with gene sets that characterize stage-specific
743 expression in parent species. For this analysis, we defined sets of overexpressed X-linked
744 diplotene genes as genes with expression (normalized FPKM) in hybrids that was in the top
745 10% of X-linked genes in parental diplotene samples (*i.e.,* genes that normally escape MSCI).
746 We then compared these sets of overexpressed hybrid diplotene genes to genes “induced” in
747 each parental stage for each species. We used DAVID v.2021 (Sherman et al. 2022) to perform
748 gene ontology (GO) analysis to identify GO terms overrepresented in differentially expressed
749 genes in hybrid samples across each cell population. We only included the longest genes
750 associated with mouse orthologs in our GO analysis, and for our background gene lists, we
751 used genes that were “expressed” in both hybrid and parent species in a given stage.
752 Biological Process GO terms with FDR below 0.05 were retained as significant. Finally, to test
753 whether specific chromosomes were enriched for differentially expressed genes for a given
754 stage, we performed hypergeometric tests on the number of differentially expressed genes on
755 a given chromosome with phyper and adjusted P-values to an FDR of 5%.
756

757 **Characterizing the behavior of PAR genes in dwarf hamsters**

758 We sought to characterize the regulatory behavior of PAR genes in dwarf hamster
759 parent species and hybrids to determine if (1) PAR genes are normally silenced in parent
760 species and (2) if PAR genes were overexpressed in hybrids (consistent with an extension of

761 MSCI to the PAR). The PAR on the *P. sungorus* X chromosome is on the distal arm of the X
762 chromosome from around 115,350,000-119,112,095 bp (Moore et al. 2022). There are 15
763 annotated *P. sungorus* genes in this region (Table S3), which is comparable to the latest PAR
764 assembly in C57BL/6J house mice (Kasahara et al. 2022). Six of these are orthologous to
765 annotated genes in mice (*Tppp2*, *Gprin1*, *Ndrg2*, *Kcnip4*, *Ndrg2*, and *Hs6st3*), but they are not
766 located in the mouse PAR (Kasahara et al. 2022). Only seven of the annotated genes in the
767 PAR were expressed in more than three replicates across all samples (Psun_G000022875,
768 Psun_G000022880, Psun_G000022883, Psun_G000022886, *Tppp2*, *Gprin1*, and *Ndrg2*). For
769 these genes, we assessed whether these genes were consistently expressed or silenced in
770 parent species at any cell stage and whether any genes were differentially expressed between
771 hybrids and either parent species at any cell stage.

Acknowledgements:

This work was supported by a National Science Foundation Graduate Research Fellowship to KEH (DGE-2034612) and the following grants awarded to KEH: Sigma Xi Grant-in-aid of Research, American Society of Mammalogists Grant-in-Aid of Research Grant, and a Society for the Study of Evolution R.C. Lewontin Early Award. Additionally, this work was supported by grants from the Eunice Kennedy Shriver National Institute of Child Health and Human Development of the National Institutes of Health (R01-HD073439, R01-HD094787) to JMG, and the National Science Foundation to ELL (DEB-2012041). We would like to thank members of the Larson, Velotta, and Good Labs for feedback on this project, Ivan Kovanda for support using the University of Denver Research Data Analysis Cluster, and Pamela K. Shaw and the UM Fluorescence Cytometry Core supported by an Institutional Development Award from the NIGMS (P30GM103338). Any opinions, findings, and conclusions or recommendations expressed in this material are those of the author(s) and do not necessarily reflect the views of the National Science Foundation or the National Institutes of Health.

Author contributions:

KEH, JMG, and ELL conceived of the study. CC, SK, ELL, and KEH conducted lab work. KEH conducted the analyses. KEH and ELL wrote the manuscript with input from ECM, CC, SK, and JMG.

Data accessibility:

The data reported in this paper are available through the National Center for Biotechnology Information under accession number PRJNA1024468. The code used for the analyses is available from GitHub (https://github.com/KelsieHunnicutt/dwarf_hamster_hybrids).

795 **LITERATURE CITED**

796 Abe H, Yeh Y-H, Munakata Y, Ishiguro K-I, Andreassen PR, Namekawa SH. 2022. Active DNA
797 damage response signaling initiates and maintains meiotic sex chromosome inactivation.
798 Nat. Commun. 13:7212.

799 Anders S, Huber W. 2010. Differential expression analysis for sequence count data. Nature
800 Precedings:1–1.

801 Barreto FS, Pereira RJ, Burton RS. 2015. Hybrid dysfunction and physiological compensation
802 in gene expression. Mol. Biol. Evol. 32:613–622.

803 Bayes JJ, Malik HS. 2009. Altered heterochromatin binding by a hybrid sterility protein in
804 Drosophila sibling species. Science 326:1538–1541.

805 Benjamini Y, Hochberg Y. 1995. Controlling the false discovery rate: a practical and powerful
806 approach to multiple testing. J. R. Stat. Soc. 57:289–300.

807 Bhattacharyya T, Gregorova S, Mihola O, Anger M, Sebestova J, Denny P, Simecek P, Forejt J.
808 2013. Mechanistic basis of infertility of mouse intersubspecific hybrids. Proc. Natl. Acad.
809 Sci. U. S. A. 110:E468–E477.

810 Bikchurina TI, Tishakova KV, Kizilova EA, Romanenko SA, Serdyukova NA, Torgasheva AA,
811 Borodin PM. 2018. Chromosome synapsis and recombination in male-sterile and female-
812 fertile interspecies hybrids of the dwarf hamsters (Phodopus, Cricetidae). Genes 9:227.

813 Bolger AM, Lohse M, Usadel B. 2014. Trimmomatic: a flexible trimmer for Illumina sequence
814 data. Bioinformatics 30:2114–2120.

815 Bredemeyer KR, Seabury CM, Stickney MJ, McCarrey JR, vonHoldt BM, Murphy WJ. 2021.

816 Rapid macrosatellite evolution promotes X-linked hybrid male sterility in a feline
817 interspecies cross. Mol. Biol. Evol. 38:5588–5609.

818 Brekke TD, Good JM. 2014. Parent-of-origin growth effects and the evolution of hybrid
819 inviability in dwarf hamsters. Evolution 68:3134–3148.

820 Brekke TD, Moore EC, Campbell-Staton SC, Callahan CM, Cheviron ZA, Good JM. 2021. X
821 chromosome-dependent disruption of placental regulatory networks in hybrid dwarf
822 hamsters. Genetics 218:iyab043.

823 Brekke TD, Steele KA, Mulley JF. 2018. Inbred or outbred? Genetic diversity in laboratory
824 rodent colonies. G3 8:679–686.

825 Burgoyne PS. 1982. Genetic homology and crossing over in the X and Y chromosomes of
826 mammals. Hum. Genet. 61:85–90.

827 Burgoyne PS, Mahadevaiah SK, Turner JMA. 2009. The consequences of asynapsis for
828 mammalian meiosis. Nat. Rev. Genet. 10:207–216.

829 Campbell P, Good JM, Nachman MW. 2013. Meiotic sex chromosome inactivation is disrupted
830 in sterile hybrid male house mice. Genetics 193:819–828.

831 Civetta A. 2016. Misregulation of gene expression and sterility in interspecies hybrids: causal
832 links and alternative hypotheses. J. Mol. Evol. 82:176–182.

833 Coughlan JM, Matute DR. 2020. The importance of intrinsic postzygotic barriers throughout
834 the speciation process. Philos. Trans. R. Soc. Lond. B Biol. Sci. 375:20190533.

835 Coyne JA, Orr HA. 1989. Two rules of speciation. In: Otte D, Endler JA, editors. Speciation and
836 its consequences. Sunderland, MA: Sinauer Associates. p. 180–207.

837 Cutter AD. 2012. The polymorphic prelude to Bateson-Dobzhansky-Muller incompatibilities.
838 Trends Ecol. Evol. 27:209–218.

839 Cutter AD, Bundus JD. 2020. Speciation and the developmental alarm clock. Elife 9:e56276.

840 Davies B, Gupta Hinch A, Cebrian-Serrano A, Alghadban S, Becker PW, Biggs D, Hernandez-
841 Pliego P, Preece C, Moralli D, Zhang G, et al. 2021. Altering the binding properties of
842 PRDM9 partially restores fertility across the species boundary. Mol. Biol. Evol. 38:5555–
843 5562.

844 Davies B, Hatton E, Altemose N, Hussin JG, Pratto F, Zhang G, Hinch AG, Moralli D, Biggs D,
845 Diaz R, et al. 2016. Re-engineering the zinc fingers of PRDM9 reverses hybrid sterility in
846 mice. Nature 530:171–176.

847 Davis BW, Seabury CM, Brashear WA, Li G, Roelke-Parker M, Murphy WJ. 2015. Mechanisms
848 underlying mammalian hybrid sterility in two feline interspecies models. Mol. Biol. Evol.
849 32:2534–2546.

850 Dumont BL. 2017. Meiotic consequences of genetic divergence across the murine
851 pseudoautosomal region. Genetics 205:1089–1100.

852 Ellis N, Goodfellow PN. 1989. The mammalian pseudoautosomal region. Trends Genet. 5:406–
853 410.

854 Forejt J, Jansa P, Parvanov E. 2021. Hybrid sterility genes in mice (Mus musculus): a peculiar
855 case of PRDM9 incompatibility. Trends Genet. 37:1095–1108.

856 Forejt J, Vincek V, Klein J, Lehrach H, Loudová-Micková M. 1991. Genetic mapping of the t-
857 complex region on mouse chromosome 17 including the Hybrid sterility-1 gene. Mamm.

858 Genome 1:84–91.

859 Gamperl R, Vistorin G, Rosenkranz W. 1977. New observations on the karyotype of the
860 Djungarian hamster, Phodopus sungorus. Experientia 33:1020–1021.

861 Getun IV, Torres B, Bois PRJ. 2011. Flow cytometry purification of mouse meiotic cells. J. Vis.
862 Exp.:e2602.

863 Good JM, Giger T, Dean MD, Nachman MW. 2010. Widespread over-expression of the X
864 chromosome in sterile F1 hybrid mice. PLoS Genet. 6:e1001148.

865 Good JM, Handel MA, Nachman MW. 2008. Asymmetry and polymorphism of hybrid male
866 sterility during the early stages of speciation in house mice. Evolution 62:50–65.

867 Green CD, Ma Q, Manske GL, Shami AN, Zheng X, Marini S, Moritz L, Sultan C, Gurczynski SJ,
868 Moore BB, et al. 2018. A comprehensive roadmap of murine spermatogenesis defined by
869 single-cell RNA-Seq. Dev. Cell 46:651–667.e10.

870 Guerrero RF, Posto AL, Moyle LC, Hahn MW. 2016. Genome-wide patterns of regulatory
871 divergence revealed by introgression lines. Evolution 70:696–706.

872 Gu Z, Eils R, Schlesner M. 2016. Complex heatmaps reveal patterns and correlations in
873 multidimensional genomic data. Bioinformatics 32:2847–2849.

874 Haaf T, Weis H, Schmid M. 1987. A comparative cytogenetic study on the mitotic and meiotic
875 chromosomes in hamster species of the genus Phodopus (Rodentia, Cricetinae).
876 Zeitschrift für Säugetierkunde 52:281–290.

877 Haerty W, Singh RS. 2006. Gene regulation divergence is a major contributor to the evolution
878 of Dobzhansky-Muller incompatibilities between species of Drosophila. Mol. Biol. Evol.

879 23:1707–1714.

880 Haldane JBS. 1922. Sex ratio and unisexual sterility in hybrid animals. J. Genet. 12:101–109.

881 Handel MA. 2004. The XY body: a specialized meiotic chromatin domain. Exp. Cell Res.
882 296:57–63.

883 Hermann BP, Cheng K, Singh A, Roa-De La Cruz L, Mutoji KN, Chen I-C, Gildersleeve H, Lehle
884 JD, Mayo M, Westernströer B, et al. 2018. The mammalian spermatogenesis single-cell
885 transcriptome, from spermatogonial stem cells to spermatids. Cell Rep. 25:1650–1667.e8.

886 Holt J, Huang S, McMillan L, Wang W. 2013. Read annotation pipeline for high-throughput
887 sequencing data. In: Proceedings of the International Conference on Bioinformatics,
888 Computational Biology and Biomedical Informatics - BCB'13. New York, New York, USA:
889 ACM Press. p. 605–612.

890 Homolka D, Ivanek R, Capkova J, Jansa P, Forejt J. 2007. Chromosomal rearrangement
891 interferes with meiotic X chromosome inactivation. Genome Res. 17:1431–1437.

892 Huang S, Holt J, Kao C-Y, McMillan L, Wang W. 2014. A novel multi-alignment pipeline for
893 high-throughput sequencing data. Database 2014:bau057.

894 Hunnicutt KE, Good JM, Larson EL. 2022. Unraveling patterns of disrupted gene expression
895 across a complex tissue. Evolution 76:275–291.

896 Ishishita S, Tsuboi K, Ohishi N, Tsuchiya K, Matsuda Y. 2015. Abnormal pairing of X and Y sex
897 chromosomes during meiosis I in interspecific hybrids of Phodopus campbelli and *P.*
898 *sungorus*. Sci. Rep. 5:9435.

899 Kasahara T, Mekada K, Abe K, Ashworth A, Kato T. 2022. Complete sequencing of the mouse

900 pseudoautosomal region, the most rapidly evolving “chromosome.”
901 bioRxiv:2022.03.26.485930.

902 Kim D, Paggi JM, Park C, Bennett C, Salzberg SL. 2019. Graph-based genome alignment and
903 genotyping with HISAT2 and HISAT-genotype. Nat. Biotechnol. 37:907–915.

904 Kopania EEK, Larson EL, Callahan C, Keeble S, Good JM. 2022. Molecular evolution across
905 mouse spermatogenesis. Mol. Biol. Evol. 39:msac023.

906 Kopania EEK, Watson EM, Rathje CC, Skinner BM, Ellis PJI, Larson EL, Good JM. 2022. The
907 contribution of sex chromosome conflict to disrupted spermatogenesis in hybrid house
908 mice. Genetics 222:iyac151.

909 Kousathanas A, Halligan DL, Keightley PD. 2014. Faster-X adaptive protein evolution in house
910 mice. Genetics 196:1131–1143.

911 Lafon-Placette C, Köhler C. 2015. Epigenetic mechanisms of postzygotic reproductive isolation
912 in plants. Curr. Opin. Plant Biol. 23:39–44.

913 Landeen EL, Muirhead CA, Wright L, Meiklejohn CD, Presgraves DC. 2016. Sex chromosome-
914 wide transcriptional suppression and compensatory cis-regulatory evolution mediate gene
915 expression in the Drosophila male germline. PLoS Biol. 14:e1002499.

916 Larson EL, Keeble S, Vanderpool D, Dean MD, Good JM. 2017. The composite regulatory
917 basis of the large X-effect in mouse speciation. Mol. Biol. Evol. 34:282–295.

918 Larson EL, Kopania EEK, Good JM. 2018. Spermatogenesis and the evolution of mammalian
919 sex chromosomes. Trends Genet. 34:722–732.

920 Larson EL, Kopania EEK, Hunnicutt KE, Vanderpool D, Keeble S, Good JM. 2022. Stage-

921 specific disruption of X chromosome expression during spermatogenesis in sterile house
922 mouse hybrids. G3 12:jkab407.

923 Larson EL, Vanderpool D, Keeble S, Zhou M, Sarver BAJ, Smith AD, Dean MD, Good JM.
924 2016. Contrasting levels of molecular evolution on the mouse X chromosome. Genetics
925 203:1841–1857.

926 Liao Y, Smyth GK, Shi W. 2014. featureCounts: an efficient general purpose program for
927 assigning sequence reads to genomic features. Bioinformatics 30:923–930.

928 Lifschytz E, Lindsley DL. 1972. The role of X-chromosome inactivation during
929 spermatogenesis. Proc. Natl. Acad. Sci. U. S. A. 69:182–186.

930 Llopart A. 2012. The rapid evolution of X-linked male-biased gene expression and the large-X
931 effect in Drosophila yakuba, D. santomea, and their hybrids. Mol. Biol. Evol. 29:3873–
932 3886.

933 Luo H, Mipam T, Wu S, Xu C, Yi C, Zhao W, Chai Z, Chen X, Wu Z, Wang J, et al. 2022. DNA
934 methylome of primary spermatocyte reveals epigenetic dysregulation associated with male
935 sterility of cattleyak. Theriogenology 191:153–167.

936 Lustyk D, Kinský S, Ullrich KK, Yancoskie M, Kašíková L, Gergelits V, Sedlacek R, Chan YF,
937 Odenthal-Hesse L, Forejt J, et al. 2019. Genomic structure of Hstx2 modifier of Prdm9-
938 dependent hybrid male sterility in mice. Genetics 213:1047–1063.

939 Mack KL, Campbell P, Nachman MW. 2016. Gene regulation and speciation in house mice.
940 Genome Res. 26:451–461.

941 Mack KL, Nachman MW. 2017. Gene regulation and speciation. Trends Genet. 33:68–80.

942 Matsuda Y, Hirobe T, Chapman VM. 1991. Genetic basis of X-Y chromosome dissociation and
943 male sterility in interspecific hybrids. Proc. Natl. Acad. Sci. U. S. A. 88:4850–4854.

944 McCarthy DJ, Chen Y, Smyth GK. 2012. Differential expression analysis of multifactor RNA-
945 Seq experiments with respect to biological variation. Nucleic Acids Res. 40:4288–4297.

946 McKee BD, Handel MA. 1993. Sex chromosomes, recombination, and chromatin conformation.
947 Chromosoma 102:71–80.

948 McManus CJ, Coolon JD, Duff MO, Eipper-Mains J, Graveley BR, Wittkopp PJ. 2010.
949 Regulatory divergence in Drosophila revealed by mRNA-seq. Genome Res. 20:816–825.

950 Meiklejohn CD, Coolon JD, Hartl DL, Wittkopp PJ. 2014. The roles of cis- and trans-regulation
951 in the evolution of regulatory incompatibilities and sexually dimorphic gene expression.
952 Genome Res. 24:84–95.

953 Michalak P, Noor MAF. 2003. Genome-wide patterns of expression in Drosophila pure species
954 and hybrid males. Mol. Biol. Evol. 20:1070–1076.

955 Mihola O, Trachtulec Z, Vlcek C, Schimenti JC, Forejt J. 2009. A mouse speciation gene
956 encodes a meiotic histone H3 methyltransferase. Science 323:373–375.

957 Mipam T, Chen X, Zhao W, Zhang P, Chai Z, Yue B, Luo H, Wang J, Wang H, Wu Z, et al.
958 2023. Single-cell transcriptome analysis and in vitro differentiation of testicular cells reveal
959 novel insights into male sterility of the interspecific hybrid cattle-yak. BMC Genomics
960 24:149.

961 Montgomery SH, Mank JE. 2016. Inferring regulatory change from gene expression: the
962 confounding effects of tissue scaling. Mol. Ecol. 25:5114–5128.

963 Moore EC, Thomas GWC, Mortimer S, Kopania EEK, Hunnicutt KE, Clare-Salzler ZJ, Larson
964 EL, Good JM. 2022. The evolution of widespread recombination suppression on the dwarf
965 hamster (Phodopus) X chromosome. Genome Biol. Evol. 14:evac080.

966 Morgan AP, Bell TA, Crowley JJ, Pardo-Manuel de Villena F. 2019. Instability of the
967 pseudoautosomal boundary in house mice. Genetics 212:469–487.

968 Morgan K, Harr B, White MA, Payseur BA, Turner LM. 2020. Disrupted gene networks in
969 subfertile hybrid house mice. Mol. Biol. Evol. 37:1547–1562.

970 Mugal CF, Wang M, Backström N, Wheatcroft D, Ålund M, Sémon M, McFarlane SE, Dutoit L,
971 Qvarnström A, Ellegren H. 2020. Tissue-specific patterns of regulatory changes underlying
972 gene expression differences among Ficedula flycatchers and their naturally occurring F1
973 hybrids. Genome Res. 30:1727–1739.

974 Murat F, Mbengue N, Winge SB, Trefzer T, Leushkin E, Sepp M, Cardoso-Moreira M, Schmidt
975 J, Schneider C, Mößinger K, et al. 2023. The molecular evolution of spermatogenesis
976 across mammals. Nature 613:308–316.

977 Namekawa SH, Park PJ, Zhang L-F, Shima JE, McCarrey JR, Griswold MD, Lee JT. 2006.
978 Postmeiotic sex chromatin in the male germline of mice. Curr. Biol. 16:660–667.

979 Neumann K, Michaux J, Lebedev V, Yigit N, Colak E, Ivanova N, Poltoraus A, Surov A, Markov
980 G, Maak S, et al. 2006. Molecular phylogeny of the Cricetinae subfamily based on the
981 mitochondrial cytochrome b and 12S rRNA genes and the nuclear vWF gene. Mol.
982 Phylogenet. Evol. 39:135–148.

983 Ogle D, Ogle MD. 2017. Package “FSA.” CRAN Repos:1–206.

984 Oka A, Mita A, Takada Y, Koseki H, Shiroishi T. 2010. Reproductive isolation in hybrid mice
985 due to spermatogenesis defects at three meiotic stages. Genetics 186:339–351.

986 Oka A, Shiroishi T. 2014. Regulatory divergence of X-linked genes and hybrid male sterility in
987 mice. Genes Genet. Syst. 89:99–108.

988 Oka A, Takada T, Fujisawa H, Shiroishi T. 2014. Evolutionarily diverged regulation of X-
989 chromosomal genes as a primal event in mouse reproductive isolation. PLoS Genet.
990 10:e1004301.

991 Oksanen J, Blanchet FG, Kindt R, Legendre P, Minchin PR, O'hara RB, Simpson GL, Solymos
992 P, Stevens MHH, Wagner H, et al. 2013. Package "vegan." Community ecology package,
993 version 2:1–295.

994 Oliver PL, Goodstadt L, Bayes JJ, Birtle Z, Roach KC, Phadnis N, Beatson SA, Lunter G, Malik
995 HS, Ponting CP. 2009. Accelerated evolution of the Prdm9 speciation gene across diverse
996 metazoan taxa. PLoS Genet. 5:e1000753.

997 Ortíz-Barrientos D, Counterman BA, Noor MAF. 2007. Gene expression divergence and the
998 origin of hybrid dysfunctions. Genetica 129:71–81.

999 Paun O, Fay MF, Soltis DE, Chase MW. 2007. Genetic and epigenetic alterations after
1000 hybridization and genome doubling. Taxon 56:649–656.

1001 Presgraves DC. 2008. Sex chromosomes and speciation in Drosophila. Trends Genet. 24:336–
1002 343.

1003 Ramm SA, Schärer L. 2014. The evolutionary ecology of testicular function: size isn't
1004 everything. Biol. Rev. Camb. Philos. Soc. 89:874–888.

1005 Rappaport Y, Achache H, Falk R, Murik O, Ram O, Tzur YB. 2021. Bisection of the X
1006 chromosome disrupts the initiation of chromosome silencing during meiosis in
1007 Caenorhabditis elegans. Nat. Commun. 12:4802.

1008 Raudsepp T, Chowdhary BP. 2015. The eutherian pseudoautosomal region. Cytogenet.
1009 Genome Res. 147:81–94.

1010 Raymond CS, Murphy MW, O'Sullivan MG, Bardwell VJ, Zarkower D. 2000. Dmrt1, a gene
1011 related to worm and fly sexual regulators, is required for mammalian testis differentiation.
1012 Genes Dev. 14:2587–2595.

1013 Ritchie ME, Phipson B, Wu D, Hu Y, Law CW, Shi W, Smyth GK. 2015. limma powers
1014 differential expression analyses for RNA-sequencing and microarray studies. Nucleic Acids
1015 Res. 43:e47.

1016 Robinson MD, McCarthy DJ, Smyth GK. 2010. edgeR: a Bioconductor package for differential
1017 expression analysis of digital gene expression data. Bioinformatics 26:139–140.

1018 Sánchez-Ramírez S, Weiss JG, Thomas CG, Cutter AD. 2021. Widespread misregulation of
1019 inter-species hybrid transcriptomes due to sex-specific and sex-chromosome regulatory
1020 evolution. PLoS Genet. 17:e1009409.

1021 Scribner SJ, Wynne-Edwards KE. 1994. Disruption of body temperature and behavior rhythms
1022 during reproduction in dwarf hamsters (Phodopus). Physiol. Behav. 55:361–369.

1023 Sherman BT, Hao M, Qiu J, Jiao X, Baseler MW, Lane HC, Imamichi T, Chang W. 2022. DAVID:
1024 a web server for functional enrichment analysis and functional annotation of gene lists
1025 (2021 update). Nucleic Acids Res. 50:W216–W221.

1026 Shivaprasad PV, Dunn RM, Santos BA, Bassett A, Baulcombe DC. 2012. Extraordinary
1027 transgressive phenotypes of hybrid tomato are influenced by epigenetics and small
1028 silencing RNAs. EMBO J. 31:257–266.

1029 Smagulova F, Brick K, Pu Y, Camerini-Otero RD, Petukhova GV. 2016. The evolutionary
1030 turnover of recombination hot spots contributes to speciation in mice. Genes Dev. 30:266–
1031 280.

1032 Swanson MT, Oliveros CH, Esselstyn JA. 2019. A phylogenomic rodent tree reveals the
1033 repeated evolution of masseter architectures. Proc. Biol. Sci. 286:20190672.

1034 Taxiarchi C, Kranjc N, Kriezis A, Kyrou K, Bernardini F, Russell S, Nolan T, Crisanti A, Galizi R.
1035 2019. High-resolution transcriptional profiling of Anopheles gambiae spermatogenesis
1036 reveals mechanisms of sex chromosome regulation. Sci. Rep. 9:14841.

1037 Trachtulec Z, Mnuková-Fajdelová M, Hamvas RM, Gregorová S, Mayer WE, Lehrach HR,
1038 Vincek V, Forejt J, Klein J. 1997. Isolation of candidate hybrid sterility 1 genes by cDNA
1039 selection in a 1.1 megabase pair region on mouse chromosome 17. Mamm. Genome
1040 8:312–316.

1041 Turner JMA. 2015. Meiotic silencing in mammals. Annu. Rev. Genet. 49:395–412.

1042 Turner LM, Harr B. 2014. Genome-wide mapping in a house mouse hybrid zone reveals hybrid
1043 sterility loci and Dobzhansky-Muller interactions. Elife 3:e02504.

1044 Turner LM, White MA, Tautz D, Payseur BA. 2014. Genomic networks of hybrid sterility. PLoS
1045 Genet. 10:e1004162.

1046 Vasimuddin M, Misra S, Li H, Aluru S. 2019. Efficient architecture-aware acceleration of BWA-

1047 MEM for multicore systems. In: 2019 IEEE International Parallel and Distributed Processing
1048 Symposium (IPDPS). IEEE. p. 314–324.

1049 Viera A, Parra MT, Arévalo S, García de la Vega C, Santos JL, Page J. 2021. X chromosome
1050 inactivation during grasshopper spermatogenesis. Genes 12:1844.

1051 White MA, Ikeda A, Payseur BA. 2012. A pronounced evolutionary shift of the
1052 pseudoautosomal region boundary in house mice. Mamm. Genome 23:454–466.

1053 White MA, Stubbings M, Dumont BL, Payseur BA. 2012. Genetics and evolution of hybrid male
1054 sterility in house mice. Genetics 191:917–934.

1055 Wittkopp PJ, Haerum BK, Clark AG. 2004. Evolutionary changes in cis and trans gene
1056 regulation. Nature 430:85–88.

1057 Wu CI, Davis AW. 1993. Evolution of postmating reproductive isolation: the composite nature
1058 of Haldane's rule and its genetic bases. Am. Nat. 142:187–212.

1059 Zhu W, Hu B, Becker C, Doğan ES, Berendzen KW, Weigel D, Liu C. 2017. Altered chromatin
1060 compaction and histone methylation drive non-additive gene expression in an interspecific
1061 Arabidopsis hybrid. Genome Biol. 18:157.